CHARLES UNIVERSITY IN PRAGUE
FACULTY OF MATHEMATICS AND PHYSICS

VISCOELASTIC RESPONSE OF THE EARTH: INITIAL-VALUE APPROACH

Summary of Ph.D. Thesis
Branch: F-7 — Geophysics

LADISLAV HANYK

JULY 1999

Školící pracoviště: Univerzita Karlova v Praze (Charles University in Prague)
Matematicko-fyzikální fakulta (Faculty of Mathematics and Physics)
Katedra geofyziky (Department of Geophysics)
V Holešovičkách 2
180 00 Praha 8 – Libeň
(Czech Republic)

Doktorand: RNDr. Ladislav Hanyk
Katedra geofyziky MFF UK

Školitel: Doc. RNDr. Ondřej Čadek, CSc.
Katedra geofyziky MFF UK

Konzultanti: Doc. RNDr. Ctirad Matyska, DrSc.
Katedra geofyziky MFF UK
Prof. Dr. David A. Yuen
Minnesota Supercomputer Institute and University of Minnesota
1200 Washington Avenue South
Minneapolis MN 55415
USA

Oponenti: Prof. RNDr. Zdeněk Martinec, DrSc.
Katedra geofyziky MFF UK
Priv.-Doz. Dr. Detlef Wolf
GeoForschungsZentrum Potsdam
AB 1: Rezente Kinematik und Dynamik der Erde
Telegrafenberg A 17
D-14473 Potsdam
BRD

Předseda oborové rady: Prof. RNDr. Zdeněk Martinec, DrSc.
Katedra geofyziky MFF UK

Disertační práce byla sepsána během postgraduálního studia doktoranda
na Matematicko-fyzikální fakultě Univerzity Karlovy v Praze v letech 1991–99.

Autoreferát byl rozeslán dne 27. srpna 1999.

Obhajoba se koná dne 28. září 1999 v 9.00 hodin před komisí pro obhajoby disertačních prací v oboru *F-7 — Geofyzika* v budově MFF UK, Ke Karlovu 3, Praha 2, v místnosti č. 105.

S disertační prací je možno se seznámit na útvaru PGDS MFF UK, Ke Karlovu 3, Praha 2.

UNIVERZITA KARLOVA V PRAZE
MATEMATICKO-FYZIKÁLNÍ FAKULTA

MODELOVÁNÍ VISKOELASTICKÉ ODEZVY ZEMĚ

Autoreferát disertační práce
Obor: F-7 — Geofyzika

LADISLAV HANYK

ČERVENEC 1999

Abstract

We have developed a new approach for the computation of temporal responses of viscoelastic Earth models to a surface load. Mathematically it is a reformulation of evolutional partial differential equations governing the infinitesimal response of the pre-stressed viscoelastic continuum into the form of an initial-value problem for ordinary differential equations. In the first part of the thesis we derive the initial-value formulation in full detail. We begin from the field partial differential equations, continue with the spherical harmonic decomposition and the spatial semi-discretization via the method of lines and discuss routines appropriate for numerical solution to resulting stiff ordinary differential equations. We also touch our older initial-value formulation based on an alternative technique of discretization. We concentrate on models with spherically symmetric distribution of physical parameters, although a set of differential equations for the case of axisymmetric viscosity is derived, too. In the second part we collect our publications on the initial-value approach. We focus on characteristic features of responses of realistic models with complex viscosity profiles. In particular, the influences of elastic compressibility, of the thickness of the lithosphere, of the nature of internal mantle boundaries and of the structure of the asthenosphere are studied. The comparison of results obtained by the initial-value and normal-mode approaches is conducted for simplified as well as for realistic models. We demonstrate the gravitational instability of a compressible homogeneous sphere. The initial-value approach offers the alternative fundamentals for the numerical modelling of the viscoelastic responses. Besides its applicability to arbitrarily stratified spherical Earth models, it provides the possibility of generalization for models with 2-D and 3-D viscosity distribution. Due to the efficiency of numerical procedures applicable to the forward problem, it can eventually extend the throughput of the inverse modelling.

Contents

Introduction

The relevance of the viscoelastic approximation of the Earth responses emerges in the context of processes operating on the transient temporal scales, between the domains of purely elastic and viscous modelling. Modelling of the uplift of regions deglaciated during the late Pleistocene epoch is the leading application. The forward problem of the postglacial rebound consists of the evaluation of response functions to the unit load and the convolution of the responses with models of glacial-oceanic loading in time and space. It is a long-standing tradition to evade the time dependence of the responses by reformulation of the problem in the Laplace domain and to express the Laplace spectra of the responses in terms of normal modes (Peltier 1974; Wu & Peltier 1982). However, the messy structure of the Laplace spectra of spherical compressible models with realistic distribution of physical parameters poses a serious obstacle for the inverse transformation of the responses back into the time domain (Han & Wahr 1995; Fang & Hager 1995). For this reason, the application of the normal-mode approach to these compressible Earth models becomes rather ineffective, if not impossible.

In the presented thesis we provide a review of our formulations of the initial-value approach to the modelling of viscoelastic responses of the Earth, from the original version by Hanyk et al. (1995, 1996) through the integro-differential formulation by Hanyk et al. (1998) up to recently discovered and here first published formulation based on the method of lines. We collect a system of field partial differential equations (PDEs) governing the global response of a spherically symmetric, gravitating, compressible Earth model to surface loading. With the elastic constitutive relation considered first, the field PDEs are converted into a system of ordinary differential equations (ODEs) with respect to the radius by means of the spherical harmonic analysis and the technique of scalar representation of both vectors and second-order tensors. Then we switch to the constitutive relation of the Maxwell viscoelasticity which introduces the time evolution into the system. We derive a linear first-order system of PDEs with respect to both time and the radius for the Maxwell solid; PDEs for the standard linear solid and for the axisymmetric viscosity distribution are found too. Next we discretize the derived PDEs for the Maxwell solid in the spatial dimension and obtain a system of ODEs with respect to time, suitable for efficient numerical implementation of stiff integrators. The Rosenbrock and semi-implicit extrapolating stiff integrators are discussed and adapted for the band-diagonal structure of the matrix of the system. Numerical properties of the new formulation are demonstrated on some examples. In the second half of the thesis we incorporate four publications which apply the initial-value approach to a large family of viscoelastic Earth models. We focus on characteristic features of responses of realistic models with complex viscosity profiles. In particular, the influence of elastic compressibility, the thickness of the lithosphere, the nature of internal mantle boundaries and the viscosity structure of the asthenosphere are studied. The comparison of results obtained by the both approaches is conducted for simplified as well as for realistic models. Finally the gravitational instability of a compressible homogeneous sphere is examined (Hanyk et al. 1999). In appendices of the thesis a survey of features of scalar spherical harmonics is given, scalar representation of scalar, vector and second-order tensor fields subjected to differential operators is derived and some perhaps useful excerpts of Fortran routines are attached.

1 Initial-Value Approach via the Method of Lines

1.1 Field Partial Differential Equations

We consider a gravitating, compressible, non-rotating continuum initially in hydrostatic equilibrium. It is conventional to decompose total fields, such as the stress tensor and the gravitational potential, into initial and incremental parts. The incremental fields are employed for description of infinitesimal, quasi-static, gravitational-viscoelastic perturbations of the initial fields. Physical quantities and field equations given below conform to the standard form of gravitational viscoelastodynamics (Peltier 1974), also referred to as the material-local form of the linearized field theory (Wolf 1997).

The initial state of the continuum is described, in terms of the initial (Cauchy) stress tensor $\boldsymbol{\tau}_0$, the initial gravitational potential φ_0, the initial density distribution ϱ_0 and the forcing term $\boldsymbol{f}_0$, by the momentum and Poisson equations, respectively,

$$\nabla \cdot \boldsymbol{\tau}_0 + \boldsymbol{f}_0 = \mathbf{0}\,, \tag{1}$$

$$\nabla^2 \varphi_0 - 4\pi G \varrho_0 = 0\,, \tag{2}$$

where G is the Newton gravitational constant. Boundary conditions required at the surface and all internal boundaries are the continuity of the normal initial stress, $[\boldsymbol{n} \cdot \boldsymbol{\tau}_0]^+_- = 0$, of the gravitational potential, $[\varphi_0]^+_- = 0$, and of the normal component of its gradient, $[\boldsymbol{n} \cdot \nabla\varphi_0]^+_- = 0$, where $\boldsymbol{n}$ is the outward unit normal with respect to the boundary; moreover, the tangential stress should vanish at liquid boundaries and at the surface, $\boldsymbol{n} \cdot \boldsymbol{\tau}_0 = (\boldsymbol{n} \cdot \boldsymbol{\tau}_0 \cdot \boldsymbol{n})\boldsymbol{n}$. The premise of the hydrostatic initial stress requires no deviatoric stresses, $\boldsymbol{\tau}_0 = -p_0 \boldsymbol{I}$, with p_0 the mechanical pressure and $\boldsymbol{I}$ the unit diagonal tensor. We take the force $\boldsymbol{f}_0$ equal to the gravity force per unit volume, $\boldsymbol{f}_0 = -\rho_0 \nabla\varphi_0$. In the case of the spherically symmetric density, $\varrho_0(r)$, where r is the radius, all initial fields also become spherically symmetric. Introducing the gravitational acceleration $g_0(r)$ by the relation $g_0 \boldsymbol{e}_r = \nabla\varphi_0$, eqs (1)–(2) reduce to

$$p_0' + \varrho_0 g_0 = 0\,, \tag{3}$$

$$g_0' + 2g_0/r - 4\pi G \varrho_0 = 0\,, \tag{4}$$

where the prime $'$ denotes differentiation with respect to r.

The incremental fields include the displacement $\mathbf{u}$, the incremental (Cauchy) stress tensor $\boldsymbol{\tau}$, the incremental gravitational potential φ_1 and the incremental density ϱ_1. Note that the incremental potential φ_1 under the presence of a surface load is due to both the gravitational forcing of the load and the internal mass redistribution of the model. For incremental fields the adoption of the concept of Lagrangian or Eulerian formulations of a field becomes necessary, the former relating the current value of a field at the material point to the initial position of that point, the latter relating the field to the current, local position. Leaving derivation of the following equations for specialized monographs (e.g., Wolf 1997), we state that if $\boldsymbol{\tau}$ is in Lagrangian description and φ_1 and ϱ_1 are in Eulerian description, then, within this rather conventional casting, the incremental field equations for infinitesimal, quasi-static perturbations, i.e., the momentum and Poisson equations, and the constitutive relation of Maxwell viscoelasticity will take the form as follows:

$$\nabla \cdot \boldsymbol{\tau} + \boldsymbol{f} = \mathbf{0}\,, \qquad \boldsymbol{f} = -\varrho_0 \nabla\varphi_1 + \nabla \cdot (\varrho_0 \mathbf{u}) g_0 \boldsymbol{e}_r - \nabla(\varrho_0 g_0 \boldsymbol{e}_r \cdot \mathbf{u})\,, \tag{5}$$

$$\nabla \cdot (\nabla\varphi_1 + 4\pi G \varrho_0 \mathbf{u}) = 0\,, \tag{6}$$

$$\dot{\boldsymbol{\tau}} = \dot{\boldsymbol{\tau}}^E - \xi\,(\boldsymbol{\tau} - K\nabla\cdot\mathbf{u}\boldsymbol{I})\,, \tag{7}$$
$$\boldsymbol{\tau}^E = \lambda\nabla\cdot\mathbf{u}\boldsymbol{I} + \mu[\nabla\mathbf{u} + (\nabla\mathbf{u})^T] \tag{8}$$

with λ and μ the elastic Lamé parameters, $K = \lambda + \frac{2}{3}\mu$ the bulk modulus, η the dynamic viscosity, $\xi = \mu/\eta$ and $\boldsymbol{\tau}^E$ the elastic part of the stress tensor. The dots above quantities denote differentiation with respect to time t. The internal boundary conditions for the incremental fields require continuity of the displacement, the incremental stress, the incremental gravitational potential and its gradient, $[\mathbf{u}]^+_- = \mathbf{0}$, $[\boldsymbol{\tau}]^+_- = \mathbf{0}$, $[\varphi_1]^+_- = 0$ and $[\nabla\varphi_1]^+_- = \mathbf{0}$, and zero tangential stress at liquid boundaries, $\boldsymbol{n}\cdot\boldsymbol{\tau} = (\boldsymbol{n}\cdot\boldsymbol{\tau}\cdot\boldsymbol{n})\boldsymbol{n}$. Under the presence of the load prescribed by the interface density γ_L, the surface boundary conditions for the incremental stress and gradient of the incremental gravitational potential balance the applied load, $[\boldsymbol{n}\cdot\boldsymbol{\tau}]^+_- = -g_0\gamma_L\boldsymbol{n}$ and $[\boldsymbol{n}\cdot(\nabla\varphi_1 + 4\pi G\rho_0\mathbf{u})]^+_- = -4\pi G\gamma_L$.

1.2 Spherical Harmonic Decomposition

Let $\boldsymbol{e}_r$, $\boldsymbol{e}_\vartheta$ and $\boldsymbol{e}_\varphi$ be the unit basis vectors of the spherical coordinates r, ϑ and φ. We introduce the scalar spherical harmonics $Y_{nm}(\vartheta,\varphi)$,

$$Y_{nm}(\vartheta,\varphi) = (-1)^m N_{nm} P_n^m(\cos\vartheta) e^{im\varphi}\,, \qquad N_n = \sqrt{\frac{2n+1}{4\pi}}\,, \tag{9}$$

where $P_n^m(\cos\vartheta)$ are the associated Legendre functions and N_{nm} the norm factors, and the vector spherical harmonics $\boldsymbol{S}^{(-1)}_{nm}$, $\boldsymbol{S}^{(1)}_{nm}$ and $\boldsymbol{S}^{(0)}_{nm}$,

$$\boldsymbol{S}^{(-1)}_{nm}(\vartheta,\varphi) = Y_{nm}\boldsymbol{e}_r\,, \tag{10}$$
$$\nabla_\Omega Y_{nm} \equiv \boldsymbol{S}^{(1)}_{nm}(\vartheta,\varphi) = \partial_\vartheta Y_{nm}\boldsymbol{e}_\vartheta + (\sin\vartheta)^{-1}\partial_\varphi Y_{nm}\boldsymbol{e}_\varphi\,, \tag{11}$$
$$\boldsymbol{e}_r\times\nabla_\Omega Y_{nm} \equiv \boldsymbol{S}^{(0)}_{nm}(\vartheta,\varphi) = -(\sin\vartheta)^{-1}\partial_\varphi Y_{nm}\boldsymbol{e}_\vartheta + \partial_\vartheta Y_{nm}\boldsymbol{e}_\varphi\,. \tag{12}$$

We can write the following expansions of the scalar and vector functions $\mathbf{u}$, φ_1, $\boldsymbol{T}_r \equiv \boldsymbol{e}_r\cdot\boldsymbol{\tau}$ and $\boldsymbol{T}^E_r \equiv \boldsymbol{e}_r\cdot\boldsymbol{\tau}^E$,

$$\mathbf{u} = \textstyle\sum_{nm}[U_{nm}(r)\boldsymbol{S}^{(-1)}_{nm} + V_{nm}(r)\boldsymbol{S}^{(1)}_{nm} + W_{nm}(r)\boldsymbol{S}^{(0)}_{nm}]\,, \tag{13}$$
$$\nabla\cdot\mathbf{u} = \textstyle\sum_{nm} X_{nm}(r)Y_{nm}\,, \tag{14}$$
$$\varphi_1 = \textstyle\sum_{nm} F_{nm}(r)Y_{nm}\,, \tag{15}$$
$$\boldsymbol{T}_r = \textstyle\sum_{nm}[T_{rr,nm}(r)\boldsymbol{S}^{(-1)}_{nm} + T_{r\vartheta,nm}(r)\boldsymbol{S}^{(1)}_{nm} + T_{r\varphi,nm}(r)\boldsymbol{S}^{(0)}_{nm}]\,, \tag{16}$$
$$\boldsymbol{T}^E_r = \textstyle\sum_{nm}[T^E_{rr,nm}(r)\boldsymbol{S}^{(-1)}_{nm} + T^E_{r\vartheta,nm}(r)\boldsymbol{S}^{(1)}_{nm} + T^E_{r\varphi,nm}(r)\boldsymbol{S}^{(0)}_{nm}]\,. \tag{17}$$

Expansions of $\nabla\cdot\boldsymbol{\tau}^E$, $\boldsymbol{f}$ and $\nabla\cdot(\nabla\varphi_1 + 4\pi G\varrho_0\mathbf{u})$ and expressions for X_{nm}, $T^E_{rr,nm}$, $T^E_{r\vartheta,nm}$, $T^E_{r\varphi,nm}$ and an auxiliary variable Q_{nm} are derived in the thesis.

1.3 Ordinary Differential Equations for the SNREI Earth

The spherically symmetric, non-rotating, elastic, isotropic (SNREI) Earth model is considered in this paragraph. We introduce vector $\mathbf{y}^E_{nm}$,

$$\mathbf{y}^E_{nm}(r) = \left(U_{nm}, V_{nm}, T^E_{rr,nm}, T^E_{r\vartheta,nm}, F_{nm}, Q_{nm}, W_{nm}, T^E_{r\varphi,nm}\right)^T\,, \tag{18}$$

with the 8 elements collected to allow trivial decomposition into the spheroidal (elements 1..6) and toroidal (elements 7..8) parts; the spheroidal elements are ordered in accord with Peltier (1974).

After application of (13)–(17) in the field PDEs (5)–(6) with (8) and by substitution of $\mathbf{y}^E_{nm}$ into both the decomposed PDEs and the expressions for $T^E_{rr,nm}$, $T^E_{r\vartheta,nm}$, $T^E_{r\varphi,nm}$ and Q_{nm}, as is shown in the thesis, we arrive at a linear first-order system of ODEs with respect to r,

$$\mathbf{y}^{E\,\prime}_{nm}(r) \;=\; \boldsymbol{A}_n(r)\mathbf{y}^E_{nm}(r)\,, \tag{19}$$

with matrix $\boldsymbol{A}_n(r)$ equal to

$$\boldsymbol{A}_n = \begin{pmatrix}
-\frac{2\lambda}{r\beta} & \frac{N\lambda}{r\beta} & \frac{1}{\beta} & 0 & 0 & 0 & 0 & 0 \\
-\frac{1}{r} & \frac{1}{r} & 0 & \frac{1}{\mu} & 0 & 0 & 0 & 0 \\
\frac{4\gamma}{r^2}-\frac{4\varrho_0 g_0}{r} & -\frac{2N\gamma}{r^2}+\frac{N\varrho_0 g_0}{r} & -\frac{4\mu}{r\beta} & \frac{N}{r} & -\frac{(n+1)\varrho_0}{r} & \varrho_0 & 0 & 0 \\
-\frac{2\gamma}{r^2}+\frac{\varrho_0 g_0}{r} & \frac{N\gamma+(N-2)\mu}{r^2} & -\frac{\lambda}{r\beta} & -\frac{3}{r} & \frac{\varrho_0}{r} & 0 & 0 & 0 \\
-4\pi G\varrho_0 & 0 & 0 & 0 & -\frac{n+1}{r} & 1 & 0 & 0 \\
-4\pi G\frac{(n+1)\varrho_0}{r} & 4\pi G\frac{N\varrho_0}{r} & 0 & 0 & 0 & \frac{n-1}{r} & 0 & 0 \\
0 & 0 & 0 & 0 & 0 & 0 & \frac{1}{r} & \frac{1}{\mu} \\
0 & 0 & 0 & 0 & 0 & 0 & \frac{(N-2)\mu}{r^2} & -\frac{3}{r}
\end{pmatrix}, \tag{20}$$

and $\beta = \lambda + 2\mu$, $\gamma = \mu(3\lambda+2\mu)/\beta = 3\mu K/\beta$ and $N = n(n+1)$. In the case of material incompressibility, $K \to \infty$, the following expressions should be considered instead:

$$1/\beta \to 0\,, \quad \lambda/\beta \to 1\,, \quad \text{and} \quad \gamma \to 3\mu\,. \tag{21}$$

System (19) is decoupled with respect to both degree n and order m, and for each n and m consists of two independent systems, one with 6×6 matrix $(a_{1..6,1..6})$, connecting the spheroidal coefficients of $\mathbf{u}$ and $\boldsymbol{\tau}^E$, and another with 2×2 matrix $(a_{7..8,7..8})$, containing the toroidal coefficients. Moreover, matrix $\boldsymbol{A}_n(r)$ is independent of m. The spherical harmonic representation of the surface boundary conditions for the point mass load, $\gamma_L(\vartheta) = \sum_n \Gamma_n P_{n0}(\cos\vartheta)$ (Farrell 1972), reads

$$\begin{pmatrix} y_3(a) \\ y_4(a) \\ y_6(a) \\ y_8(a) \end{pmatrix} = \frac{1}{N_n}\begin{pmatrix} -g_0\Gamma_n \\ 0 \\ -4\pi G\Gamma_n \\ 0 \end{pmatrix}, \qquad \Gamma_n = \frac{2n+1}{4\pi a^2}\,, \tag{22}$$

where a is the radius of the Earth and the norm factors N_n come from (9).

1.4 Partial Differential Equations for the Maxwell Solid

In this paragraph we reformulate the problem of gravitational viscoelastodynamics purely in the time domain. As a starting point we recall the constitutive relation of the Maxwell rheology,

$$\dot{\boldsymbol{\tau}} \;=\; \dot{\boldsymbol{\tau}}^E - \xi\left(\boldsymbol{\tau} - K\nabla\cdot\mathbf{u}\boldsymbol{I}\right), \tag{23}$$

with $\xi = \mu/\eta$, and the field PDEs in the form

$$\nabla \cdot \dot{\boldsymbol{\tau}}^E + \dot{\boldsymbol{f}} = \nabla \cdot \left[\xi \left(\boldsymbol{\tau} - K \nabla \cdot \mathbf{u} \boldsymbol{I} \right) \right] , \tag{24}$$

$$\nabla \cdot (\nabla \varphi_1 + 4\pi G \varrho_0 \mathbf{u}) = 0 . \tag{25}$$

We consider the spatial distribution of the parameters and field variables as follows:

$$\varrho_0 = \varrho_0(r) , \quad \lambda = \lambda(r) , \quad \mu = \mu(r) , \quad K = K(r) , \quad g_0 = g_0(r) , \quad \eta = \eta(r) , \quad \xi = \xi(r) , \tag{26}$$

$$\mathbf{u} = \mathbf{u}(r, \vartheta, \varphi) , \quad \varphi_1 = \varphi_1(r, \vartheta, \varphi) , \quad \boldsymbol{\tau} = \boldsymbol{\tau}(r, \vartheta, \varphi) . \tag{27}$$

The solution vector $\mathbf{y}_{nm}(t, r)$ can be constructed from the coefficients of the spherical harmonic expansions of $\mathbf{u}$, φ_1 and $\boldsymbol{\tau}$ similarly as $\mathbf{y}^E_{nm}$ in (18),

$$\mathbf{y}_{nm}(t, r) = (U_{nm}, V_{nm}, T_{rr,nm}, T_{r\vartheta,nm}, F_{nm}, Q_{nm}, W_{nm}, T_{r\varphi,nm})^T . \tag{28}$$

Vectors $\mathbf{y}_{nm}$ and $\mathbf{y}^E_{nm}$ differ in the stress components, related in accordance with (23),

$$\dot{\boldsymbol{T}}_r = \dot{\boldsymbol{T}}^E_r - \xi \left(\boldsymbol{T}_r - K \nabla \cdot \mathbf{u} \, \boldsymbol{e}_r \right) . \tag{29}$$

The steps to be undertaken are similar to those outlined in the previous paragraph; a resulting system of PDEs is to be expressed in terms of $\mathbf{y}_{nm}$ instead of $\mathbf{y}^E_{nm}$. We arrive at a linear first-order system of PDEs with respect to time and the radius for the solution vector $\mathbf{y}_{nm}$,

$$\dot{\mathbf{y}}'_{nm}(t, r) - \boldsymbol{A}_n(r) \dot{\mathbf{y}}_{nm}(t, r) = \xi \begin{pmatrix} a_{13}(y_3 - KX) \\ a_{24} y_4 \\ -y'_3 + b_{33}(y_3 - KX) + b_{34} y_4 + \sum_k c_{3k} y_k \\ -y'_4 + b_{43}(y_3 - KX) + b_{44} y_4 + \sum_k c_{4k} y_k - KX/r \\ 0 \\ 0 \\ a_{78} y_8 \\ -y'_8 + b_{88} y_8 \end{pmatrix} , \tag{30}$$

which can be rewritten into the form

$$\dot{\mathbf{y}}'_{nm}(t, r) - \boldsymbol{A}_n(r) \dot{\mathbf{y}}_{nm}(t, r) = \xi(r) \left[\boldsymbol{D}_n(r) \mathbf{y}'_{nm}(t, r) + \boldsymbol{E}_n(r) \mathbf{y}_{nm}(t, r) \right] . \tag{31}$$

Matrix $\boldsymbol{A}_n(r)$ keeps the form of (20) and the explicit expressions of matrices $\boldsymbol{D}_n(r)$ and $\boldsymbol{E}_n(r)$ follow from (30) after substitution of expressions for coefficients X, a_{ik}, b_{ik} and c_{ik}, which can be found in the thesis,

$$\boldsymbol{D}_n = \begin{pmatrix} -\frac{K}{\beta} & 0 & 0 & 0 & 0 & 0 & 0 & 0 \\ 0 & 0 & 0 & 0 & 0 & 0 & 0 & 0 \\ \frac{4\gamma}{3r} & 0 & -1 & 0 & 0 & 0 & 0 & 0 \\ -\frac{2\gamma}{3r} & 0 & 0 & -1 & 0 & 0 & 0 & 0 \\ 0 & 0 & 0 & 0 & 0 & 0 & 0 & 0 \\ 0 & 0 & 0 & 0 & 0 & 0 & 0 & 0 \\ 0 & 0 & 0 & 0 & 0 & 0 & 0 & 0 \\ 0 & 0 & 0 & 0 & 0 & 0 & 0 & -1 \end{pmatrix} , \tag{32}$$

$$\boldsymbol{E}_n = \begin{pmatrix} -\frac{2K}{r\beta} & \frac{NK}{r\beta} & \frac{1}{\beta} & 0 & 0 & 0 & 0 & 0 \\ 0 & 0 & 0 & \frac{1}{\mu} & 0 & 0 & 0 & 0 \\ \frac{8\gamma}{3r^2} - \frac{4\varrho_0 g_0}{r} & -\frac{4N\gamma}{3r^2} + \frac{N\varrho_0 g_0}{r} & -\frac{4\mu}{r\beta} & \frac{N}{r} & -\frac{(n+1)\varrho_0}{r} & \varrho_0 & 0 & 0 \\ -\frac{4\gamma}{3r^2} + \frac{\varrho_0 g_0}{r} & \frac{2N\gamma}{3r^2} & -\frac{\lambda}{r\beta} & -\frac{3}{r} & \frac{\varrho_0}{r} & 0 & 0 & 0 \\ 0 & 0 & 0 & 0 & 0 & 0 & 0 & 0 \\ 0 & 0 & 0 & 0 & 0 & 0 & 0 & 0 \\ 0 & 0 & 0 & 0 & 0 & 0 & 0 & \frac{1}{\mu} \\ 0 & 0 & 0 & 0 & 0 & 0 & 0 & -\frac{3}{r} \end{pmatrix}. \quad (33)$$

Similarly as in the elastic case, system (31) is separated with respect to both n and m and matrices $\boldsymbol{A}_n$, $\boldsymbol{D}_n$ and $\boldsymbol{E}_n$ remain independent of m and consist of 6×6 spheroidal and 2×2 toroidal blocks.

In order to treat PDEs (31) as an initial-value problem, one needs to specify the initial condition, e.g., the value of $\mathbf{y}_{nm}(t, r)$ for $t = 0$. Here we consider the point mass load with the Heaviside dependence in time, i.e., the point mass load applied at the surface, $r = a$, in the time instant $t = 0$ and effecting continuously for $t > 0$. The Maxwell Earth responds elastically in the time instant of the load application, thus, the appropriate initial condition is $\mathbf{y}_{nm}(0, r) = \mathbf{y}^E_{nm}(r)$. The surface boundary conditions for this load keep the form of (22) uniformly for $t \geq 0$. Note that with the surface boundary conditions due to the point mass load, the spheroidal part of the system only needs to be solved. At internal solid boundaries the continuity of all elements of $\mathbf{y}_{nm}(t, r)$ is required, and at liquid boundaries the boundary conditions are according to, e.g., Wu & Peltier (1982). At $r = 0$, finite values of $\mathbf{y}_{nm}$ are expected. To find the initial condition for a spherically symmetric model with arbitrary distribution of density and elastic parameters, ODEs (19) must be solved numerically. However, for the homogeneous Earth model the solutions are known analytically and these analytical solutions can be employed in numerical integration for arbitrarily stratified models as the starting solutions. Hence, we rewrite here explicitly three independent solutions to (19) for a compressible model (λ finite) with constant values of ϱ_0, λ and μ (Wu & Peltier 1982),

$$\mathbf{y}_1 = \begin{pmatrix} -\frac{NCj_n(kr) + krj'_n(kr)}{k^2 r} \\ -\frac{(1+C)j_n(kr) + Ckrj'_n(kr)}{k^2 r} \\ \lambda j_n(kr) + 2\mu\left[\frac{NC}{kr}\left(\frac{j_n(kr)}{kr} - j'_n(kr)\right) - j''_n(kr)\right] \\ -\mu C j_n(kr) + 2\mu\left[\frac{1+C}{kr}\left(\frac{j_n(kr)}{kr} - j'_n(kr)\right) - Cj''_n(kr)\right] \\ \frac{3\varsigma j_n(kr)}{k^2} \\ \frac{3\varsigma(1-nC)(1+n)j_n(kr)}{k^2 r} \end{pmatrix}, \quad \mathbf{y}_3 = \begin{pmatrix} nr^{n-1} \\ r^{n-1} \\ 2\mu n(n-1)r^{n-2} \\ 2\mu(n-1)r^{n-2} \\ -n\varsigma r^n \\ -2n(n-1)\varsigma r^{n-1} \end{pmatrix}, \quad (34)$$

where $\varsigma = \frac{4}{3}\pi G\varrho_0$, $N = n(n+1)$ and j_n, j'_n and j''_n are the spherical Bessel functions with the first and second derivatives, respectively. The subscripts n and m of $\mathbf{y}_{nm}$ have been suppressed. Solution vector $\mathbf{y}_2$ preserves the form of $\mathbf{y}_1$ with k replaced by q and C by D where

$$2k^2 = \frac{4\varsigma\varrho_0}{\beta} + \sqrt{\left(\frac{4\varsigma\varrho_0}{\beta}\right)^2 + \frac{4N\varsigma^2\varrho_0^2}{\mu\beta}}\,, \qquad 2q^2 = \frac{4\varsigma\varrho_0}{\beta} - \sqrt{\left(\frac{4\varsigma\varrho_0}{\beta}\right)^2 + \frac{4N\varsigma^2\varrho_0^2}{\mu\beta}}\,, \tag{35}$$

$$C = -\frac{\varsigma\varrho_0}{\mu k^2}\,, \qquad D = -\frac{\varsigma\varrho_0}{\mu q^2}\,, \tag{36}$$

with $\beta = \lambda + 2\mu$.

1.5 Partial Differential Equations for the Standard Linear Solid

In order to demonstrate the applicability of the initial-value approach to other viscoelastic rheologies, we derive a system of PDEs for the spherically symmetric Earth responding like the standard linear solid. We consider the constitutive relation in the form (Peltier 1982)

$$\dot{\boldsymbol{\tau}} + \frac{\mu 1 + \mu 2}{\eta}\left(\boldsymbol{\tau} - \frac{1}{3}\bar{\boldsymbol{\tau}}\,\boldsymbol{I}\right) = \lambda\,\dot{\bar{\boldsymbol{e}}}\,\boldsymbol{I} + 2\mu_1\,\dot{\boldsymbol{e}} + \frac{2\mu_1\mu_2}{\eta}\left(\boldsymbol{e} - \frac{1}{3}\bar{\boldsymbol{e}}\,\boldsymbol{I}\right)\,, \tag{37}$$

where λ and μ_1 are the elastic Lamé parameters, μ_2 and η are the shear modulus and the viscosity associated with the Kelvin-Voight element and $\bar{\boldsymbol{\tau}}$ and $\bar{\boldsymbol{e}}$ are the first invariants of the stress and strain tensors, respectively. We invoke the auxiliary parameters $\xi_1 = (\mu_1 + \mu_2)/\eta$ and $\xi_2 = 2\mu_1\mu_2/\eta$ with the physical units s^{-1} and $\mathrm{Pa\,s}^{-1}$, respectively. Repeating the derivation similar to that made for the Maxwell solid, we obtain PDEs with respect to time and the radius for the solution vector $\mathbf{y}_{nm}$ with the rheology of the standard linear solid in the form essentially identical with (31),

$$\begin{aligned}\dot{\mathbf{y}}'_{nm}(t,r) - \boldsymbol{A}_n(r)\dot{\mathbf{y}}_{nm}(t,r) &= \xi_1(r)\left[\boldsymbol{D}_n(r)\mathbf{y}'_{nm}(t,r) + \boldsymbol{E}_n(r)\mathbf{y}_{nm}(t,r)\right] \\ &+ \xi_2(r)\left[\boldsymbol{F}_n(r)\mathbf{y}'_{nm}(t,r) + \boldsymbol{G}_n(r)\mathbf{y}_{nm}(t,r)\right]\,.\end{aligned} \tag{38}$$

Matrices $\boldsymbol{A}_n$, $\boldsymbol{D}_n$ and $\boldsymbol{E}_n$ (with μ replaced by μ_1) are given by (20), (32) and (33), respectively, and explicit expressions for matrices $\boldsymbol{F}_n$ and $\boldsymbol{G}_n$ follow from what is given in the thesis.

1.6 Partial Differential Equations for the Axisymmetric Viscoelastic Earth

The derivation of PDEs (31) for the responses of the spherically symmetric, Maxwell Earth model to a surface load can be generalized to conform with the axially symmetric (2-D) distribution of viscosity; on the contrary, we must enforce the restrictive assumption of the axial geometry of the load with identical axes of symmetry of both the viscosity and the load. Then, the spatial dependence of the viscoelastic response of this system is axisymmetric as well. We consider the following spatial distribution of the parameters and the field variables,

$$\varrho_0 = \varrho_0(r)\,, \quad \lambda = \lambda(r)\,, \quad \mu = \mu(r)\,, \quad K = K(r)\,, \quad g_0 = g_0(r)\,, \quad \eta = \eta(r,\vartheta)\,, \quad \xi = \xi(r,\vartheta)\,, \tag{39}$$

$$\mathbf{u} = \mathbf{u}(r,\vartheta)\,, \quad \varphi_1 = \varphi_1(r,\vartheta)\,, \quad \boldsymbol{\tau} = \boldsymbol{\tau}(r,\vartheta)\,. \tag{40}$$

We introduce the scalar and vector zonal spherical harmonics, Y_n and $\boldsymbol{S}_n^{(-1)}$, $\boldsymbol{S}_n^{(1)}$, $\boldsymbol{S}_n^{(0)}$, respectively, and the derivatives Z_n of Y_n, all the functions of the colatitude ϑ only,

$$Y_n(\vartheta) = Y_{n0}\,, \quad Z_n(\vartheta) = \partial_\vartheta Y_{n0}\,, \tag{41}$$

$$\boldsymbol{S}_n^{(-1)}(\vartheta) = Y_n\boldsymbol{e}_r\,, \quad \boldsymbol{S}_n^{(1)}(\vartheta) = Z_n\boldsymbol{e}_\vartheta\,, \quad \boldsymbol{S}_n^{(0)}(\vartheta) = Z_n\boldsymbol{e}_\varphi\,. \tag{42}$$

The spherical harmonic expansions (13), (15) and (16) of $\mathbf{u}$, φ_1, $\boldsymbol{T}_r$ and of the stress vector $\boldsymbol{T}_\vartheta \equiv \boldsymbol{e}_\vartheta \cdot \boldsymbol{\tau}$ are reduced to

$$\begin{aligned}
\mathbf{u}(r,\vartheta) &= \textstyle\sum_n [U_n(r) Y_n \boldsymbol{e}_r + V_n(r) Z_n \boldsymbol{e}_\vartheta + W_n(r) Z_n \boldsymbol{e}_\varphi] , && (43)\\
\varphi_1(r,\vartheta) &= \textstyle\sum_n F_n(r) Y_n , && (44)\\
\boldsymbol{T}_r(r,\vartheta) &= \textstyle\sum_n [T_{rr,n}(r) Y_n \boldsymbol{e}_r + T_{r\vartheta,n}(r) Z_n \boldsymbol{e}_\vartheta + T_{r\varphi,n}(r) Z_n \boldsymbol{e}_\varphi] , && (45)\\
\boldsymbol{T}_\vartheta(r,\vartheta) &= \textstyle\sum_n [T_{\vartheta r,n}(r) Y_n \boldsymbol{e}_r + T_{\vartheta\vartheta,n}(r) Z_n \boldsymbol{e}_\vartheta + T_{\vartheta\varphi,n}(r) Z_n \boldsymbol{e}_\varphi] , && (46)
\end{aligned}$$

analogically for the elastic parts of the stress vectors, $\boldsymbol{T}_r^E \equiv \boldsymbol{e}_r \cdot \boldsymbol{\tau}^E$ and $\boldsymbol{T}_\vartheta^E \equiv \boldsymbol{e}_\vartheta \cdot \boldsymbol{\tau}^E$. The relations between the stress vectors and the corresponding elastic parts follow from the Maxwell constitutive relation (23),

$$\begin{aligned}
\dot{\boldsymbol{T}}_r &= \dot{\boldsymbol{T}}_r^E - \xi(r,\vartheta) \left(\boldsymbol{T}_r - K \nabla \cdot \mathbf{u}\, \boldsymbol{e}_r\right) , && (47)\\
\dot{\boldsymbol{T}}_\vartheta &= \dot{\boldsymbol{T}}_\vartheta^E - \xi(r,\vartheta) \left(\boldsymbol{T}_\vartheta - K \nabla \cdot \mathbf{u}\, \boldsymbol{e}_\vartheta\right) . && (48)
\end{aligned}$$

The solution vector $\mathbf{y}_n(t,r)$ for the case of the 2-D viscosity contains 11 elements,

$$\mathbf{y}_n(t,r) = \left(U_n, V_n, T_{rr,n}, T_{r\vartheta,n}, F_n, Q_n, W_n, T_{r\varphi,n}, \bar{T}_{\vartheta r,n}, \bar{T}_{\vartheta\vartheta,n}, \bar{T}_{\vartheta\varphi,n}\right)^T , \qquad (49)$$

with the last three elements closely related to the components of $\boldsymbol{T}_\vartheta$. Vector $\mathbf{y}_n^E(r)$ is defined analogically. We denote $\langle a; B_{n'}\rangle_{YY,n}$, $\langle a; B_{n'}\rangle_{ZY,n}$, $\langle a; B_{n'}\rangle_{YZ,n}$ and $\langle a; B_{n'}\rangle_{ZZ,n}$ the coefficients of the product $a(r,\vartheta)b(r,\vartheta)$, where $a(r,\vartheta)$ is a prescribed function and $b(r,\vartheta)$ is a function known by coefficients of its expansions in terms of either Y_n or $Z_n \sin\vartheta$,

$$\begin{aligned}
a(r,\vartheta) \textstyle\sum_n B_n(r) Y_n(\vartheta) &= \textstyle\sum_n \langle a; B_{n'}\rangle_{YY,n}(r) Y_n(\vartheta) ,\\
a(r,\vartheta) \textstyle\sum_n B_n(r) Z_n(\vartheta) \sin\vartheta &= \textstyle\sum_n \langle a; B_{n'}\rangle_{ZY,n}(r) Y_n(\vartheta) ,\\
a(r,\vartheta) \textstyle\sum_n B_n(r) Y_n(\vartheta) &= \textstyle\sum_n \langle a; B_{n'}\rangle_{YZ,n}(r) Z_n(\vartheta) \sin\vartheta ,\\
a(r,\vartheta) \textstyle\sum_n B_n(r) Z_n(\vartheta) \sin\vartheta &= \textstyle\sum_n \langle a; B_{n'}\rangle_{ZZ,n}(r) Z_n(\vartheta) \sin\vartheta .
\end{aligned} \qquad (50)$$

These coefficients can be evaluated by efficient numerical procedures. In the thesis a linear first-order system of PDEs with respect to time and the radius for the solution vector $\mathbf{y}_n$ is derived in the form of generalized PDEs (30),

$$\dot{\mathbf{y}}'_{1..8,n} - \boldsymbol{A}_n \dot{\mathbf{y}}_{1..8,n} = \begin{pmatrix}
a_{13,n}\langle \xi; y_{3,n'} - KX_{n'}\rangle_{YY,n} \\
a_{24,n}\langle \xi; y_{4,n'}\rangle_{ZZ,n} \\
-\langle \xi; y'_{3,n'}\rangle_{YY,n} + b_{33,n}\langle \xi; y_{3,n'} - KX_{n'}\rangle_{YY,n} + b_{34,n}\langle \xi; y_{4,n'}\rangle_{ZZ,n} \\
\quad + \langle \xi; \textstyle\sum_k c_{3k,n'} y_{k,n'}\rangle_{YY,n} + \langle \zeta/r; y_{9,n'}\rangle_{ZY,n} \\
-\langle \xi; y'_{4,n'}\rangle_{ZZ,n} + b_{43,n}\langle \xi; y_{3,n'} - KX_{n'}\rangle_{YY,n} + b_{44,n}\langle \xi; y_{4,n'}\rangle_{ZZ,n} \\
\quad + \langle \xi; \textstyle\sum_k c_{4k,n'} y_{k,n'} - KX_{n'}/r\rangle_{ZZ,n} + \langle \zeta/r; y_{10,n'} - KX_{n'}\rangle_{YZ,n} \\
0 \\
0 \\
a_{78,n}\langle \xi; y_{8,n'}\rangle_{ZZ,n} \\
-\langle \xi; y'_{8,n'}\rangle_{ZZ,n} + b_{88,n}\langle \xi; y_{8,n'}\rangle_{ZZ,n} + \langle \zeta/r; y_{11,n'}\rangle_{YZ,n}
\end{pmatrix} , \qquad (51)$$

$$\dot{\mathbf{y}}_{9..11,n} - \dot{\mathbf{y}}^E_{9..11,n} = \begin{pmatrix}
-\langle \xi; y_{9,n'}\rangle_{ZZ,n} \\
-\langle \xi; y_{10,n'} - KX_{n'}\rangle_{YY,n} \\
-\langle \xi; y_{11,n'}\rangle_{YY,n}
\end{pmatrix} . \qquad (52)$$

It is supplemented by the three band-diagonal systems of linear algebraic equations for $y^E_{9,n}$, $y^E_{10,n}$ and $y^E_{11,n}$,

$$t^+_{n-2}\,y^E_{9,n-2} + t^0_n y^E_{9,n} + t^-_{n+2}\,y^E_{9,n+2} = \mu\left[y'_{2,n} + (y_{1,n} - y_{2,n})/r\right], \tag{53}$$

$$\begin{aligned} s^+_{n-2}y^E_{10,n-2} + s^0_n y^E_{10,n} + s^-_{n+2}y^E_{10,n+2} &= \\ = s^+_{n-2}\left[\lambda X_{n-2} + 2\mu/r\,(y_{1,n-2} - (n-2)(n-1)y_{2,n-2})\right] + s^0_n\left[\lambda X_n + 2\mu/r\,(y_{1,n} - n(n+1)y_{2,n})\right] \\ + s^-_{n+2}\left[\lambda X_{n+2} + 2\mu/r\,(y_{1,n+2} - (n+2)(n+3)y_{2,n+2})\right] - 2\mu/r\left[z^+_{n-2}y_{2,n-2} + z^0_n y_{2,n} + z^-_{n+2}y_{2,n+2}\right], \end{aligned} \tag{54}$$

$$\begin{aligned} s^+_{n-2}y^E_{11,n-2} + s^0_n y^E_{11,n} + s^-_{n+2}y^E_{11,n+2} &= \\ = -\mu/r\left[s^+_{n-2}(n-2)(n-1)y_{7,n-2} + s^0_n n(n+1)y_{7,n} + s^-_{n+2}(n+2)(n+3)y_{7,n+2}\right] \\ - 2\mu/r\left[z^+_{n-2}y_{7,n-2} + z^0_n y_{7,n} + z^-_{n+2}y_{7,n+2}\right]. \end{aligned} \tag{55}$$

This is a differential-algebraic system of 11 PDEs and 3 algebraic equations for each degree considered; coupling among systems of close degrees is maintained through both the r.h.s. of the PDEs and the band-diagonal shape of the algebraic equations.

1.7 Method of Lines. Step 1: Discretization in Space

It is known from the normal-mode approach that the response of the Maxwell compressible Earth can be characterized by the exponential-like development in time and by the spatial distribution which can be expressed in terms of the spherical Bessel functions. In other words, the behaviour of $\mathbf{y}(t,r)$ (subscripts nm are suppressed once again) is considerably different in the directions of each independent variable. For this kind of PDEs, methods based on semi-discretization are of a great benefit. Here we discuss the semi-discretizing method referred to as the method of lines (MOL, e.g., Schiesser 1991).

Semi-discretizing methods for solution to the time- and spatially-dependent PDEs are based on decomposition of the process of discretization into two steps: discretization in space and discretization in time. Either of these steps leads first to intermediate ODEs, and second to algebraic equations. The actual sequence of the steps determines whether the intermediate ODEs form an initial-value (IV) problem or a boundary-value (BV) problem. The intent of the two-step discretization is to allow for utilization of specialized techniques designed for solution to the intermediate ODEs. These techniques accomplish the second, often trickier, or at least too routine, step of the process of solution. In order to present a compact numerical formulation of the IV/MOL approach, we discretize PDEs (31) in the spatial dimension using the second-order finite-difference (FD) formulas, although FD formulas of higher orders could be employed in a similar manner. On the arbitrarily spaced grid, $x_0 = b < x_1 < \ldots < x_J = a$, we can write the second-order FD formulas for the first derivative of $f(x)$ in the general form,

$$f'_0 \approx \beta_0 f_0 + \gamma_0 f_1 + \alpha_0 f_2\,, \tag{56}$$

$$f'_j \approx \alpha_j f_{j-1} + \beta_j f_j + \gamma_j f_{j+1}\,, \qquad j = 1, 2, \ldots, J-1\,, \tag{57}$$

$$f'_J \approx \gamma_J f_{J-2} + \alpha_J f_{J-1} + \beta_J f_J\,, \tag{58}$$

where $f_j \equiv f(x_j)$, $j = 0, \ldots, J$, and α_j, β_j and γ_j are the weights dependent on locations of the grid points. A numerical routine can be used for the evaluation of the weights (Fornberg 1996).

Let us consider PDEs (31) in an interior point x_j. With FD formulas (56)–(58), the term $\dot{\mathbf{y}}'$ is approximated by $\alpha_j\dot{\mathbf{y}}_{j-1} + \beta_j\dot{\mathbf{y}}_j + \gamma_j\dot{\mathbf{y}}_{j+1}$, similarly $\boldsymbol{D}\mathbf{y}' \approx \boldsymbol{D}_j(\alpha_j\mathbf{y}_{j-1} + \beta_j\mathbf{y}_j + \gamma_j\mathbf{y}_{j+1})$, etc.

It becomes apparent that PDEs (31) discretized with respect to r can be expressed in the form of ODEs for the solution vector $\mathbf{y}(t)$,

$$\boldsymbol{P}\dot{\mathbf{y}}(t) \quad = \quad \boldsymbol{Q}\mathbf{y}(t) + \mathbf{q}\,. \tag{59}$$

Vector $\mathbf{y}(t)$ consists of $8 \times (J+1)$ elements,

$$\mathbf{y}(t) = \left(\boxed{\mathbf{y}_0}, \boxed{\mathbf{y}_1}, \ldots, \boxed{\mathbf{y}_J} \right) , \tag{60}$$

where each block represents one 8-element vector $\mathbf{y}_j \equiv \mathbf{y}(t, r_j)$, $j = 0, \ldots, J$. Matrix $\boldsymbol{P}$ is band-diagonal with constant coefficients and made from 8×8 blocks. It can be schematically sketched in the form of $J+1$ block-rows and the same number of block-columns as follows:

$$\boldsymbol{P} = \begin{pmatrix} \boxed{\beta_0\boldsymbol{I} - \boldsymbol{A}_0} & \boxed{\gamma_0\boldsymbol{I}} & \boxed{\alpha_0\boldsymbol{I}} & & 0 \\ \boxed{\alpha_1\boldsymbol{I}} & \boxed{\beta_1\boldsymbol{I} - \boldsymbol{A}_1} & \boxed{\gamma_1\boldsymbol{I}} & & \\ & \boxed{\alpha_2\boldsymbol{I}} & \boxed{\beta_2\boldsymbol{I} - \boldsymbol{A}_2} & \boxed{\gamma_2\boldsymbol{I}} & \\ & \ddots & \ddots & \ddots & \\ & & \boxed{\alpha_{J-1}\boldsymbol{I}} & \boxed{\beta_{J-1}\boldsymbol{I} - \boldsymbol{A}_{J-1}} & \boxed{\gamma_{J-1}\boldsymbol{I}} \\ 0 & & \boxed{\gamma_J\boldsymbol{I}} & \boxed{\alpha_J\boldsymbol{I}} & \boxed{\beta_J\boldsymbol{I} - \boldsymbol{A}_J} \end{pmatrix} , \tag{61}$$

where $\boldsymbol{I}$ is the diagonal matrix and $\boldsymbol{A}_j \equiv \boldsymbol{A}(r_j)$, $j = 0, \ldots, J$. Focussing the attention to the specific, i.e., diagonal shape of the two thinly framed blocks, $\alpha_0\boldsymbol{I}$ and $\gamma_J\boldsymbol{I}$, these blocks can be eliminated by subtraction of the appropriately multiplied adjacent block-rows, i.e., those with $\gamma_1\boldsymbol{I}$ and $\alpha_{J-1}\boldsymbol{I}$, respectively. Matrix $\boldsymbol{Q}$ is band-diagonal, too, and can be sketched in a similar manner,

$$\boldsymbol{Q} = \begin{pmatrix} \boxed{\beta_0\boldsymbol{D}_0 + \boldsymbol{E}_0} & \boxed{\gamma_0\boldsymbol{D}_0} & \boxed{\alpha_0\boldsymbol{D}_0} & & 0 \\ \boxed{\alpha_1\boldsymbol{D}_1} & \boxed{\beta_1\boldsymbol{D}_1 + \boldsymbol{E}_1} & \boxed{\gamma_1\boldsymbol{D}_1} & & \\ & \boxed{\alpha_2\boldsymbol{D}_2} & \boxed{\beta_2\boldsymbol{D}_2 + \boldsymbol{E}_2} & \boxed{\gamma_2\boldsymbol{D}_2} & \\ & \ddots & \ddots & \ddots & \\ & & \boxed{\alpha_{J-1}\boldsymbol{D}_{J-1}} & \boxed{\beta_{J-1}\boldsymbol{D}_{J-1} + \boldsymbol{E}_{J-1}} & \boxed{\gamma_{J-1}\boldsymbol{D}_{J-1}} \\ 0 & & \boxed{\gamma_J\boldsymbol{D}_J} & \boxed{\alpha_J\boldsymbol{D}_J} & \boxed{\beta_J\boldsymbol{D}_J + \boldsymbol{E}_J} \end{pmatrix} , \tag{62}$$

where (sic) $\boldsymbol{D}_j \equiv \xi(r_j)\boldsymbol{D}(r_j)$ and $\boldsymbol{E}_j \equiv \xi(r_j)\boldsymbol{E}(r_j)$, $j = 0, \ldots, J$. The elimination of the off-diagonal blocks is only feasible if all corresponding elements of the adjacent blocks are mutually proportional. This has been the case of the diagonally-shaped blocks, but it might not be the case of the blocks $\alpha_0\boldsymbol{D}_0$ and $\gamma_J\boldsymbol{D}_J$ versus $\gamma_1\boldsymbol{D}_1$ and $\alpha_{J-1}\boldsymbol{D}_{J-1}$. However, a setting of $\boldsymbol{D}_0 = \boldsymbol{D}_1$ and $\boldsymbol{D}_J = \boldsymbol{D}_{J-1}$ seems to be a satisfactory approximation. The r.h.s. vector $\mathbf{q}$ has the same block structure as $\mathbf{y}(t)$ in (60); an explicit expression of $\mathbf{q}$ depends on imposed boundary conditions and is discussed in the thesis. Note that the spheroidal and toroidal parts of (59) remain decoupled and that the spheroidal part only needs to be solved when the boundary conditions (22) are considered.

1.8 Method of Lines. Step 2: Integration in Time

It is a general feature of MOL that the intermediate ODEs possess a high degree of numerical stiffness. Several classes of higher-order methods for integrating stiff ODEs (referred to as the stiff integrators) have been proposed. We describe generalizations of the Runge-Kutta method, namely the Rosenbrock methods (e.g., Press et al. 1996); a generalization of the Bulirsch-Stoer methods, also called the semi-implicit extrapolation methods, is described in the thesis. A particular reason for the choice of these integrators is the lower memory consumption than in the case of the multistep methods (based on backward differentiation formulas), what can become prohibitive in 2-D and 3-D modelling. Let us consider the ODEs

$$\dot{\boldsymbol{y}} = \boldsymbol{f}(t, \boldsymbol{y}) \,, \qquad \boldsymbol{y}(t_0) = \boldsymbol{y}_0 \,. \tag{63}$$

The general scheme of the Runge-Kutta methods for integrating (63) is

$$\boldsymbol{y}(t_0 + h) = \boldsymbol{y}_0 + \sum_{i=1}^{s} c_i \boldsymbol{k}_i \,, \qquad \boldsymbol{k}_i = h\boldsymbol{f}\left(\boldsymbol{y}_0 + \sum_{j=1}^{i-1} \alpha_{ij} \boldsymbol{k}_j\right), \quad i = 1, \ldots, s \,, \tag{64}$$

with h the stepsize and c_i and α_{ij} constants of a particular member of the Runge-Kutta family. In the Rosenbrock methods vectors $\boldsymbol{k}_i$ are solutions to s linear algebraic equations

$$(\boldsymbol{I} - \gamma h \boldsymbol{f}') \cdot \boldsymbol{k}_i = h\boldsymbol{f}\left(\boldsymbol{y}_0 + \sum_{j=1}^{i-1} \alpha_{ij} \boldsymbol{k}_j\right) + h\boldsymbol{f}' \cdot \sum_{j=1}^{i-1} \gamma_{ij} \boldsymbol{k}_j \,, \quad i = 1, \ldots, s \,, \tag{65}$$

where $\boldsymbol{f}' \equiv \partial \boldsymbol{f} / \partial \boldsymbol{y}$ denotes the Jacobian matrix and the coefficients c_i, γ, α_{ij} and γ_{ij} are constants of a particular member of the Rosenbrock family. The algorithm for the automatic stepsize adjustment in the Rosenbrock methods based on the embedded Runge-Kutta-Fehlberg schemes is implemented in Press et al. (1996).

ODEs (59) can be cast into (63) with $\boldsymbol{f} = \boldsymbol{P}^{-1}(\boldsymbol{Q}\mathbf{y} + \mathbf{q})$ and $\boldsymbol{f}' = \boldsymbol{P}^{-1}\boldsymbol{Q}$. In this case it is advisable to rewrite the Rosenbrock scheme (65) in the form of

$$(\boldsymbol{P} - \gamma h \boldsymbol{Q}) \cdot \boldsymbol{k}_i = h\left[\boldsymbol{Q}\left(\mathbf{y}_0 + \sum_{j=1}^{i-1} \alpha_{ij} \boldsymbol{k}_j\right) + \mathbf{q}\right] + h\boldsymbol{Q} \cdot \sum_{j=1}^{i-1} \gamma_{ij} \boldsymbol{k}_j \,, \quad i = 1, \ldots, s \,, \tag{66}$$

where the band-diagonal matrices appear on the both sides. We see that at each time step, one algebraic system with the matrix $\boldsymbol{P} - \gamma h \boldsymbol{Q}$ must be solved repeatedly for several different r.h.s. Matrices $\boldsymbol{P}$ and $\boldsymbol{Q}$ are constant and given by (61) and (62), respectively, vector $\mathbf{q}$ depends on imposed boundary conditions. It is a crucial property of this algebraic system that $\boldsymbol{P} - \gamma h \boldsymbol{Q}$ is a band-diagonal matrix and that band-diagonal solvers may be applied. Numerical characteristics (both processing time and required memory) thus become linear functions of the number of spatial grid points. Solvers to algebraic band-diagonal equations are available anywhere (e.g., LAPACK in *http://www.netlib.org*, or `bandec` & `banbks` accompanied with the routine `banmul` for matrix-vector multiplication on the r.h.s. by Press et al. 1996). The block structure of the diagonal band of $\boldsymbol{P} - \gamma h \boldsymbol{Q}$ allures to employ solvers which would exploit this feature. An appropriate solver to these systems with block-diagonal matrices, based on Gaussian elimination, can be also found in Press et al. (1996) in the context of solving BV problems of ODEs by relaxation methods.

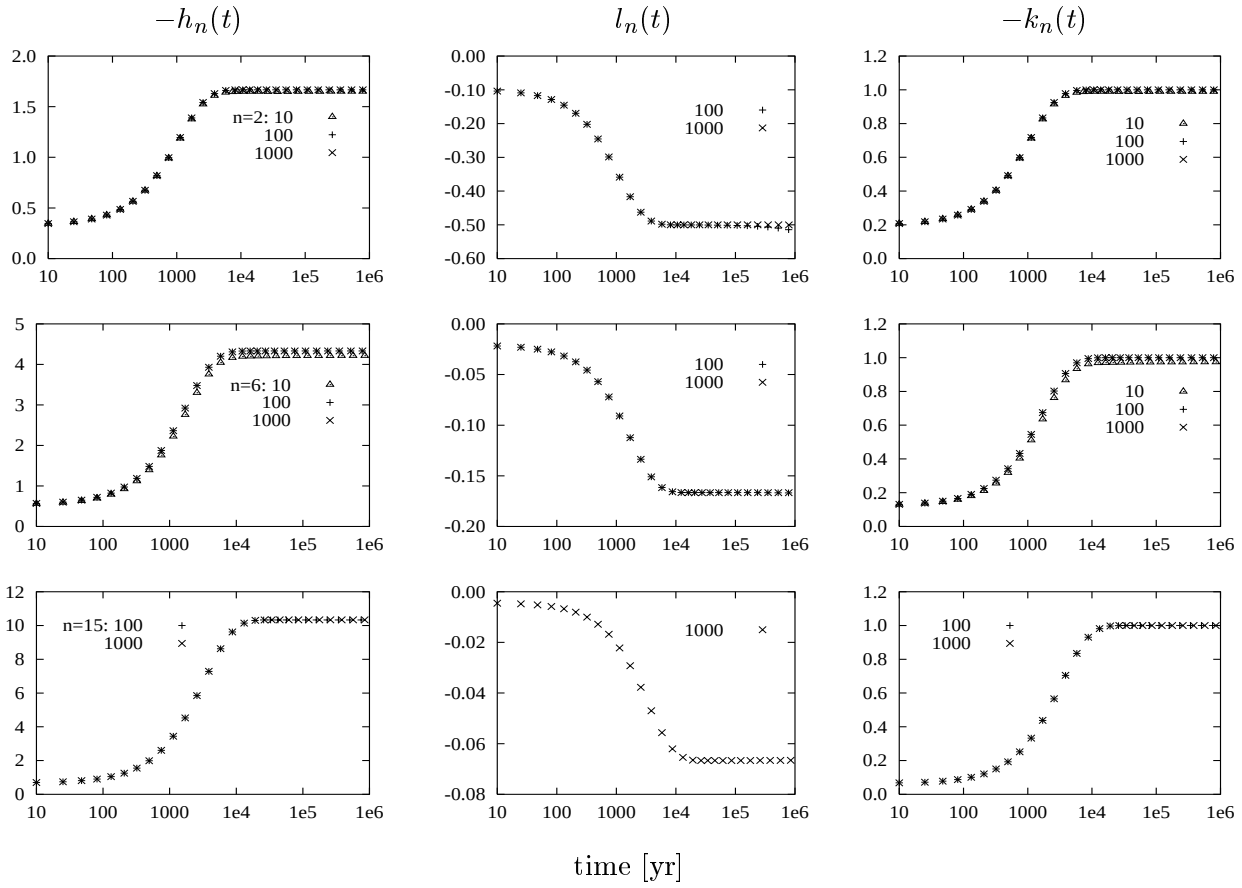

Figure 1: Time evolution of the surface Love numbers h_n, l_n and k_n, $n = 2$, 6 and 15, of the homogeneous incompressible model evaluated by the IV/MOL approach. One symbol represents one time step made by the Rosenbrock stiff integrator. The responses have been calculated with various density of the spatial discretization: symbols $\triangle$ denote values obtained with 11 equidistant spatial grid points (!), + pertain to 101 grid points and $\times$ to 1001 grid points ($J = 10$, 100 and 1000, respectively). The equilibrium state is reached with less than 20 time steps; with 101 grid points, recent Pentium processors generate 20 time steps per second.

1.9 Numerical Implementation

In order to validate the new formulation and to appraise the potential of the new code, we illustrate the IV/MOL formulation by some output of the numerical modelling. Our current implementation targets on the homogeneous, spherically symmetric, Maxwell viscoelastic Earth models, represented by the usual average Earth model (Wu & Peltier 1982). The code solves the spheroidal part of ODEs (59) with constant matrices $\boldsymbol{P}$, $\boldsymbol{Q}$ and vector $\mathbf{q}$. Spatial grid points may be distributed arbitrarily, $r_0 = b < r_1 < \ldots < r_J = a$, with a the radius of the model and b the radius of the elastic "core", underlying the viscoelastic "mantle". Boundary conditions at $r = a$ have been imposed on $\mathbf{y}_J(t) = \mathbf{y}(t, a)$ in accord with (22). ODEs (59) have been solved by the Rosenbrock stiff integrator adapted for solution to systems with band-diagonal matrices. In Fig. 1 we demonstrate the time evolution of the surface values of the Love numbers h_n, l_n and k_n, $n = 2$, 6 and 15, for the first 10^6 yr after the onset of the Heaviside (in time) point mass load at the surface. The surface Love numbers are related to the 1st, 2nd and 5th elements of $\mathbf{y}_J(t)$ by the definition (Farrell 1972)

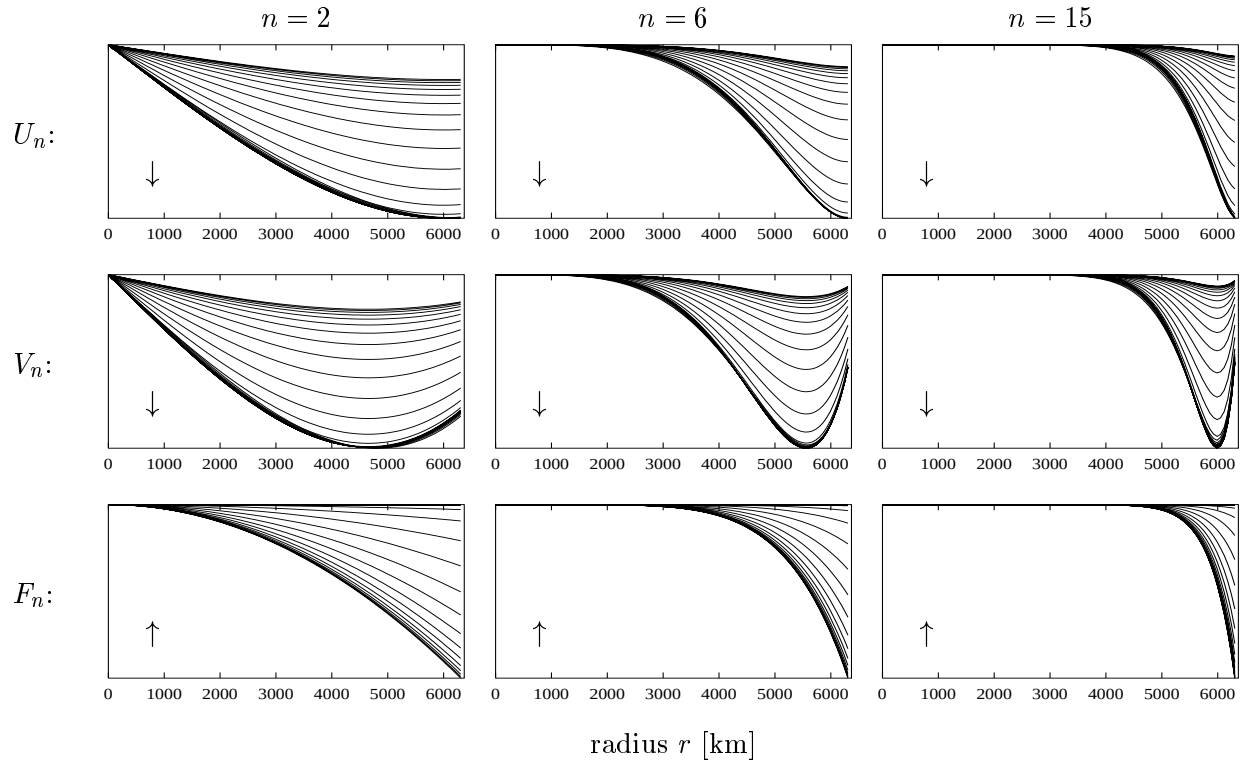

Figure 2: Time evolution of the physical components of the discretized solution vector $\mathbf{y}(t)$ of the homogeneous incompressible model from the elastic response at $t = 0$ up to $t = 10^6$ yr. The direction of the progress in time is depicted by the arrows; timing of the particular time instants can be revealed by comparison with the surface values given in Fig. 1. Spatial dimension of 6371 km has been discretized by 101 grid points. Vertical labelling is relative and has been suppressed.

$$\begin{pmatrix} y_{J,1} \\ y_{J,2} \\ y_{J,5} \end{pmatrix} = \frac{\Phi_n}{N_n} \begin{pmatrix} h_n/g_0 \\ l_n/g_0 \\ -k_n \end{pmatrix}, \quad \Phi_n = \frac{4\pi G a \Gamma_n}{2n+1}, \quad N_n = \sqrt{\frac{2n+1}{4\pi}}, \quad \Gamma_n = \frac{2n+1}{4\pi a^2}, \tag{67}$$

with Φ_n the coefficients of the spherical harmonic expansion of the surface potential of the point mass load and N_n the norm factors of the spherical harmonics, cf. (9). The long-time values of the surface Love numbers accurately fit the isostatic limits known analytically (Wu & Peltier 1982),

$$\lim_{t\to\infty} h_n(t) = -\frac{2n+1}{3}, \quad \lim_{t\to\infty} k_n(t) = -1. \tag{68}$$

Symbols $\triangle$, $+$ and $\times$ represent the time instants chosen automatically by the Rosenbrock stiff integrator; each time instant is depicted. We have employed 11, 101 and 1001 equally spaced grid points in the spatial dimension (i.e., $J = 10$, 100 and 1000, respectively). Adaptive stepsize control works satisfactorily: the state of the isostatic equilibrium has been reached within 20 time steps, and the time instant of 10^6 yr within 30 time steps. The speed of the integration is governed by the number of spatial grid points. As an example we can say that the Pentium/350 processor generates 20 time steps per second with 101 spatial grid points. Let us recall that both processing time and required memory are linear functions of the number of spatial grid points. In Fig. 2 we monitor the depth dependence of $\mathbf{y}(t)$. The time evolution of selected components of $\mathbf{y}(t)$ has been plotted in the "one time step—one curve" manner.

2 Publications on the Initial-Value Approach

2.1 Initial-Value Approach via the Method of Rothe

Our older formulation of the initial-value approach is not based on the method of lines but on an alternative semi-discretizing method, referred to as the method of Rothe (MOR, e.g., Rektorys 1982). The characteristic feature of MOR is that the discretization od PDEs in time is performed first. Although MOR does not seem to be a particularly effective method for numerical solution to differential systems with a higher degree of stiffness, results presented in our previous publications and collected in the second part of the thesis have been computed by a method equivalent to the application of MOR to PDEs (30)/(31). Let us consider the Euler first-order explicit FD formula $\dot{f}(t^i) \equiv \dot{f}^i \approx (f^{i+1} - f^i)/\Delta t^i$, where $\Delta t^i \equiv t^{i+1} - t^i$. Applying this FD formula to the time derivatives in PDEs (30), we obtain the boundary-value problem for $\mathbf{y}_n^{i+1}$, introduced by Hanyk et al. (1996),

$$(\mathbf{y}_n^{i+1})' \;=\; \boldsymbol{A}_n \mathbf{y}_n^{i+1} + \mathbf{q}_n^i \,, \tag{69}$$

where

$$\mathbf{q}_n^i \;=\; \mathbf{q}_n^{i-1} \begin{pmatrix} 1 \\ 1 \\ 1-\xi\Delta t^i \\ 1-\xi\Delta t^i \\ 0 \\ 0 \\ 1 \\ 1-\xi\Delta t^i \end{pmatrix} + \xi\Delta t^i \begin{pmatrix} \frac{1}{\beta}(y_3^i - KX^i) \\ \frac{1}{\mu} y_4^i \\ -\frac{4\gamma}{r^2} y_1^i + \frac{2N\gamma}{r^2} y_2^i + \frac{4\gamma}{3r} X^i \\ \frac{2\gamma}{r^2} y_1^i - \frac{N\gamma + (N-2)\mu}{r^2} y_2^i - \frac{2\gamma}{3r} X^i \\ 0 \\ 0 \\ \frac{1}{\mu} y_8^i \\ -\frac{(N-2)\mu}{r^2} y_7^i \end{pmatrix} . \tag{70}$$

If we consider the implicit FD formula $\dot{f}^{i+1} \approx (f^{i+1} - f^i)/\Delta t^i$, we will obtain from PDEs (31) at the time level $t = t^{i+1}$,

$$(\mathbf{y}_n^{i+1})' \;=\; \boldsymbol{A}_n \mathbf{y}_n^{i+1} + \mathbf{q}_n^{i+1} \,, \tag{71}$$

$$\mathbf{q}_n^{i+1} \;=\; \mathbf{q}_n^i + \xi\Delta t^i \left[(\boldsymbol{D}_n \boldsymbol{A}_n + \boldsymbol{E}_n) \mathbf{y}_n^{i+1} + \boldsymbol{D}_n \mathbf{q}_n^{i+1} \right] . \tag{72}$$

This system also follows from the discretized integro-differential system by Hanyk et al. (1998),

$$\mathbf{y}_n'(t,r) \;=\; \boldsymbol{A}_n(r) \mathbf{y}_n(t,r) + \mathbf{q}_n(t,r) \,, \tag{73}$$

$$\mathbf{q}_n(t,r) \;=\; \int_0^t \xi \left[\tilde{\boldsymbol{Q}}_n(r) \mathbf{y}_n(t',r) + \tilde{\tilde{\boldsymbol{Q}}}_n(r) \mathbf{q}_n(t',r) \right] dt' \,, \tag{74}$$

as is shown in the thesis.

These formulations of the IV approach have been applied to compressible Earth models with complex viscosity profiles. We have demonstrated that realistic elastically compressible models

generate an infinite number of modes and the width of such "continuous spectrum" may cover several orders of magnitude in the Laplace domain for complicated viscosity stratification. From our numerical solutions, we have directed our attention on the influences of elastic compressibility, thickness of the lithosphere, the nature of the internal mantle boundaries with density jumps and the viscosity structure near the interface between the lower and upper mantle. There is a great difference between the responses of compressible and incompressible models mainly for shorter wavelengths. We have studied the viscoelastic responses to the lithospheric thickness in the presence of a low-viscosity asthenosphere for various types of viscosity profiles and found that there are differences in the responses at short wavelengths for viscosity profiles with sharp low-viscosity zones. The sensitivity of the viscoelastic response to the nature of the internal boundaries with density jumps and viscosity jumps near the 670 km boundary are weaker but they are still noteworthy for low degrees. We have concluded that the normal-mode approach is best suited for simple layered models, long wavelengths and timescales greater than several thousand years, while the initial-value approach is indispensable in treating short-timescale problems with sharp low-viscosity zones in the upper mantle and viscosity stratification in the lower mantle.

2.2 Secular Gravitational Instability of a Compressible Viscoelastic Sphere

We have uncovered the existence of unstable modes of compressible Maxwell viscoelastic Earth models. These modes can be shown to have origins arising from the gravitational Rayleigh-Taylor instability of a compressible viscoelastic layer. Plag & Jüttner (1995) investigated numerically this kind of instability for the PREM model. We have demonstrated analytically the secular instability of a homogeneous compressible sphere. We have derived analytical expressions for the roots of the secular determinant based on analytical solutions for the homogeneous compressible sphere in the Laplace domain, cf. (34) and Wu & Peltier (1982), and on the asymptotic expansion of the spherical Bessel functions. From the secular equation in the $s \to 0_+$ limit, $\sin(k(s)r - n\pi/2) = 0$, where s is the Laplace variable, the analytical formula for the (positive) roots of the unstable Rayleigh-Taylor modes follows,

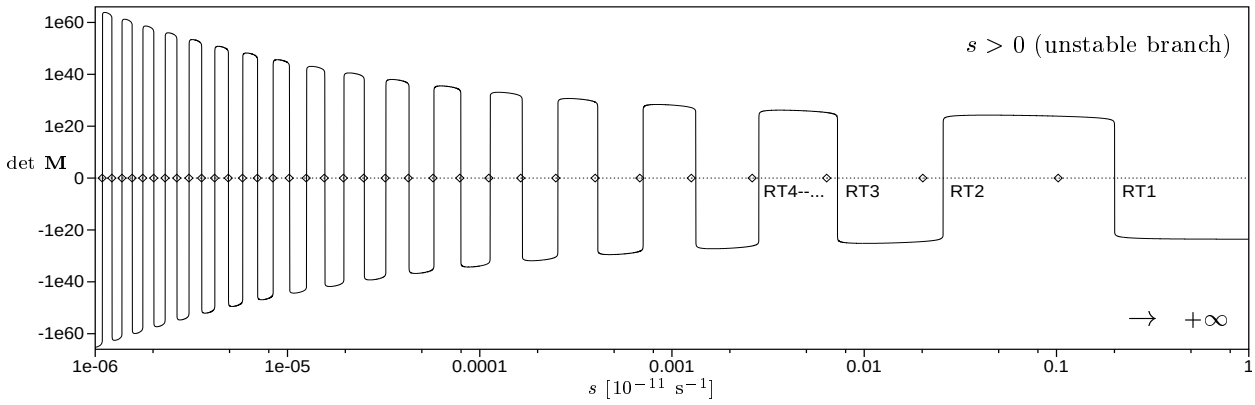

Figure 3: Secular determinant as a function of the Laplace variable s (solid lines) for the compressible homogeneous sphere. The asymptotic validity of the roots $s_n^{\mathrm{RT}m}$ by (75), corresponding to the growth times of the unstable Rayleigh-Taylor modes, is demonstrated by diamonds lying on the zero line.

$$s_n^{\mathrm{RT}m} = \frac{n(n+1)}{K\eta} \frac{\left(r^2 \rho \varsigma\right)^2}{\left[(2m+n)\frac{\pi}{2}\right]^4}\,, \tag{75}$$

with m the overtone number and $\varsigma = \frac{4}{3}\pi G \varrho_0$. Note that the incompressible sphere, $K \to \infty$, is stable. The growth times $1/s_n^{\mathrm{RT}m}$ for low m, amounting to $\mathrm{O}(10^4)$ yr for the longest wavelength, must be found numerically by root-finding procedures, the asymptotic formula (75) can, however, be considered as the analytical proof of the existence of the unstable modes. We have also refined on the previous analysis of the stable branch of the secular determinant, $s < 0$, by Vermeersen et al. (1996). It can be acknowledged that the initial-value approach has contributed to the disclosure of the secular instability of compressible spheres, the fact forgettable and sometime being forgotten in the framework of the normal-mode approach.

References

Fang, M. & Hager, B.H., 1995. The singularity mystery associated with a radially continuous Maxwell viscoelastic structure, *Geophys. J. Int.*, **123**, 849–865.

Farrell, W.E., 1972. Deformation of the earth by surface loads, *Rev. Geophys. Space Phys.*, **10**, 761–797.

Fornberg, B., 1996. *A Practical Guide to Pseudospectral Methods*, Cambridge University Press, New York.

Han, D. & Wahr, J., 1995. The viscoelastic relaxation of a realistically stratified earth, and a further analysis of postglacial rebound, *Geophys. J. Int.*, **120**, 287–311.

Hanyk, L., Matyska, C. & Yuen, D.A., 1998. Initial-value approach for viscoelastic responses of the Earth's mantle, in *Dynamics of the Ice Age Earth: A Modern Perspective*, ed. by P. Wu, pp. 135–154, Trans Tech Publ., Zürich, Switzerland.

Hanyk, L., Matyska, C. & Yuen, D.A., 1999. Secular gravitational instability of a compressible viscoelastic sphere, *Geophys. Res. Lett.*, **26**, 557–560.

Hanyk, L., Moser, J., Yuen, D.A. & Matyska, C., 1995. Time-domain approach for the transient responses in stratified viscoelastic Earth models, *Geophys. Res. Lett.*, **22**, 1285–1288.

Hanyk, L., Yuen, D.A. & Matyska, C., 1996. Initial-value and modal approaches for transient viscoelastic responses with complex viscosity profiles, *Geophys. J. Int.*, **127**, 348–362.

Peltier, W.R., 1974. The impulse response of a Maxwell earth, *Rev. Geophys. Space Phys.*, **12**, 649–669.

Peltier, W.R., 1982. Dynamics of the Ice Age earth, *Adv. Geophys.*, **24**, 1–146.

Plag, H.-P. & Jüttner, H.-U., 1995. Rayleigh-Taylor instabilities of a self-gravitating Earth, *J. Geodynamics*, **20**, 267–288.

Press, W.H., Teukolsky, S.A., Vetterling, W.T. & Flannery, B.P., 1996. *Numerical Recipes in Fortran 77: The Art of Scientific Computing*, second edition, Cambridge University Press, New York.

Rektorys, K., 1982. *The Method of Discretization in Time and Partial Differential Equations*, Reidel Publ., Dortrecht-Boston-London.

Schiesser, W.E., 1991. *The Numerical Method of Lines: Integration of Partial Differential Equations*, Academic Press, San Diego.

Vermeersen, L.L.A., Sabadini, R. & Spada, G., 1996. Compressible rotational deformation, *Geophys. J. Int.*, **126**, 735–761.

Wolf, D., 1997. Gravitational viscoelastodynamics for a hydrostatic planet, *Habilitation thesis*, Bayerische Akademie der Wissenschaften, München, Germany.

Wu, P. & Peltier, W.R., 1982. Viscous gravitational relaxation, *Geophys. J. R. astr. Soc.*, **70**, 435–485.